*17th World Conference on Earthquake Engineering, 17WCEE*

*Sendai, Japan - September 13th to 18th 2020*

# DYNAMIC INSTABILITY PHENOMENON OF CEILING SUSPENDED WITH LONG HANGING BOLTS DURING EARTHQUAKES

S. Motoyui[(1)] , Y. Sato[(2)] , T. Ohtsuka[(3)]

[(1)] *Professor, Tokyo Institute of Technology, motoyui.s.aa@m.titech.ac.jp*
[(2)] *Researcher, Takenaka Corporation, satou.yasuaki@takenaka.co.jp*
[(3)] *Associate Professor, Meijo Univeristy, Ohtsuka@meijo-u.ac.jp*

## *Abstract*

While it is possible to explain why certain types of ceilings fell during an earthquake, falling of suspended ceilings has complex causes and they are not fully understood. In order to secure room space safe, it is important to elucidate the each and every complicated cause of such ceiling fall. In the previous paper, we focused on ceiling systems suspended with long hanging bolts, and discussed in such ceiling systems, the unstable behavior of the system was considered the cause of ceiling surface falling during an earthquake. We also pointed out that the numerical analysis results show that the axial force acting on a hanging bolt changes drastically due to the dynamic instability of the hanging bolt, and such extreme change of the axial force causes the ceiling to fall. This conclusion is consistent with the fact that many ceilings suspended with long hanging bolts were damaged in earthquakes. However, some problems remain unsolved. Specifically, in the numerical model applied to dynamic instability analyses, it is assumed that both ends of the hanging bolt are simply supported. But the actual support condition is not so simple that numerical results can be completely different from the actual behavior. Furthermore, the influence of dynamic horizontal disturbance acting on the hanging bolt has not been taken into consideration. But it is inappropriate not to consider that effect since the magnitude of horizontal acceleration is larger than that of vertical one.

The first purpose of this paper is to show that the above-mentioned instability phenomenon actually occurs through shaking table tests, where we use a ceiling specimen consisting of typical details used for general JPN style ceilings. In the test, the test specimen consists of one long hanging bolt (length 3.8m) and a ceiling surface. The size of ceiling surface (about 1m$^2$) is determined so as to be equal to the standard area size supported by one hanging bolt. The input acceleration wave is a sweep wave composed of vertical acceleration only. According to results obtained by this test, a much larger axial force (about 4 times the static load) acting on the hanging bolt was observed, even though only a vertical acceleration of 0.8G maximum was input. The fact means dynamic instability also occurred in the test using an actual ceiling system. The second purpose of this paper is to experimentally clarify the effect of dynamic horizontal disturbance on the dynamic instability phenomenon of hanging bolts. In this test, a test specimen is composed of 12 long hanging bolts (length: 2.95 m, 6 hanging bolts x 2 rows). It is confirmed that the axial force on a hanging bolt changes greatly as in the case where only a dynamic vertical disturbance is applied. This phenomenon means that even when only a dynamic horizontal disturbance acts on the ceiling, a strong non-linear phenomenon occurs when the ceiling has long hanging bolts. Finally, we present the conditions under which such unstable phenomena occur on the ceiling that is subject to both vertical and horizontal disturbances.

*Keywords: Suspended ceiling; Dynamic instability; Shaking table test; Geometrical nonlinear analysis*

## 1. Introduction

In recent earthquakes, non-structural components of those buildings such as ceilings were seriously damaged as shown in Photos.1, while most structural frames were not damaged and also, the maximum acceleration values recorded at the nearby site were comparatively small. For this reason, research on seismic performance of non-structural elements has been strongly promoted in Japan, and as a result, it gradually becomes clear why certain types of ceilings fall during an earthquake [2][3]. However, though it is possible to explain why certain types of ceilings actually fell during an earthquake, falling of suspended ceilings has complex causes and they are not fully made clear. In order to secure safe room space, it is important to elucidate the each and every complicated cause of such ceiling falls. In the previous paper [1], we focused on ceiling systems suspended with long hanging bolts and reached conclusion that in such ceiling systems, the unstable behavior of the hanging bolts should be one of the causes of ceiling surface fall during an earthquake. In fact, the numerical analysis results show that axial force acting on a hanging bolt changes drastically due to dynamic instability of the hanging bolt, and such extreme change of the axial force causes the ceiling to fall. This conclusion is consistent with the fact that many ceilings suspended with long hanging bolts were damaged in earthquakes. However, some problems remain unsolvedin our suggestion. Specifically, in the numerical model applied to dynamic instability analyses, it is assumed that both ends of the hanging bolt are simply supported. But the actual support condition is not so simple that numerical results can be completely different from the actual behavior. Furthermore, the influence of dynamic horizontal disturbance acting on the hanging bolt has not been taken into consideration. But it is inappropriate not to consider that effect since the magnitude of horizontal acceleration is larger than that of vertical one.

The first purpose of this paper is to show that the above-mentioned instability phenomenon of the hanging bolt subjected to dynamic vertical disturbance actually occurs through shaking table tests, in which we use a ceiling specimen consisting of typical details used for general JPN style ceilings. The second purpose of this paper is to experimentally clarify the influence of dynamic horizontal disturbance on the dynamic instability phenomenon of hanging bolts.

We focus on JPN style ceilings in this paper. As shown in Photo.2, JPN style ceilings are quite different from US counterparts. In JPN style, a threaded rod (ordinary outer diameter: 9mm) is used as a hanging member. The top end of the hanging bolt is anchored to main structural members like slabs or girders. At its bottom, one of steel members with channel cross-section (C-38x12x1.2) is attached with 'hangers' (a metal connection parts). To that channel, another steel member called M-bar (M-25x19x0.6) is connected with 'clips' (metal connection parts). Finally, gypsum boards that form the ceiling surface are attached to M-bar with screws and this is the way JPN style ceiling is constructed.

Photos.1 Falling examples of ceiling during earthquake

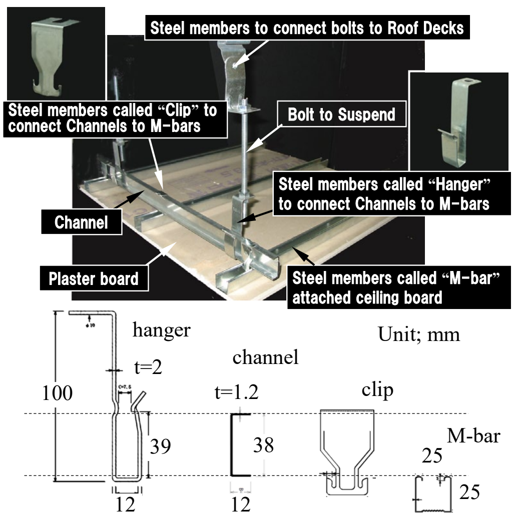


Photo.2 JPN style ceiling



 

## 2. Long hanging bolt subjected to vertical dynamic disturbance

### 2.1 Outline of test

The purpose of this experiment is to verify the validity of the results in numerical analysis shown by Motoyui [1]. As shown in Figures 1 and 2, a test specimen consists of one long hanging bolt (length 3.8m) and a ceiling surface. The size of ceiling surface (1m x 1m) is determined so as to be equal to the standard area size supported by one hanging bolt. A polycarbonate board in place of gypsum boards is used for ceiling surface, and JIS standard materials are used for steel furring. The top of the hanging bolt is supported by a pin joint. The four corners of the ceiling surface are supported by vertical rollers, allowing only vertical displacement and restraining other displacements and any rotations. The mass of the ceiling surface is used as a parameter, and the specimen with mass of 18.25 kg is *L4000 model*, and the specimen with steel plates attached to the ceiling with mass of 35.25 kg is *L4000w model*.

In order to investigate the natural frequency of the hanging bolt in the horizontal (lateral) direction, a free vibration test was conducted in which an initial displacement was given by pulling a string in the horizontal direction at the center of the hanging bolt. Figures 3(a) and (b) show the results of free vibration experiments of *L4000 model* in the *x* and *y* direction respectively. With these results, it is found that natural frequencies in the *x* and *y* directions are 2.6 3Hz and 3.00 Hz respectively. Similarly, natural frequencies in the *x* and *y* directions of *L4000w model* are 3.45 Hz and 3.80 Hz respectively. The damping constant *h* is obtained by drawing a damping curve on the amplitude of the accelerometer during free vibration. The damping constants obtained this way are 0.8% for x direction and 3.0% for y direction in both models. Next, in order to grasp ~~the~~ natural frequency in the vertical direction, a vertical standing wave excitation experiment is carried out. Figure 4 shows the relationship between the axial force on the hanging bolt and the vertical displacement of the ceiling surface when a 2.0Hz, 8m/s$^2$ stationary wave was input. In Figure 4, the vertical stiffness of this test specimen is 1800 N/mm, and by substituting its value into a formula for a natural frequency of single DOF, natural frequencies of *L4000* and *L4000w* models are calculated to be 50 Hz and 36 Hz. Since these values of frequency are much higher than the natural frequency in the horizontal direction, these two modes are quite independent from each other in the linear deformation level.

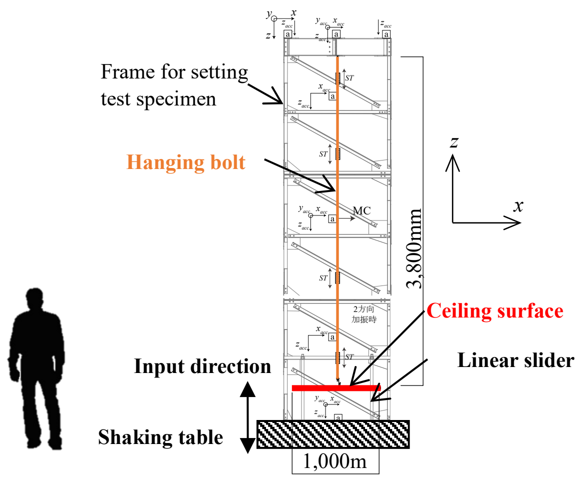


Fig.1 Test apparatus

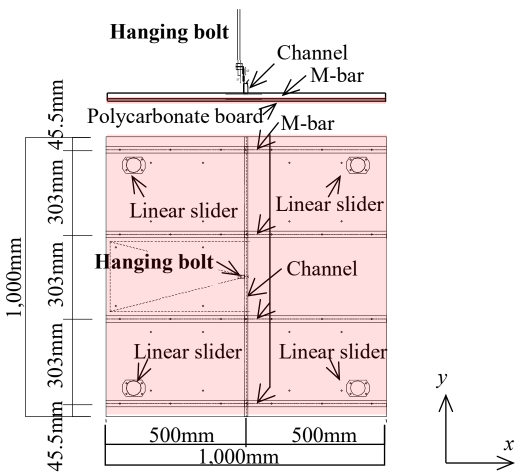


Fig.2 Test specimen

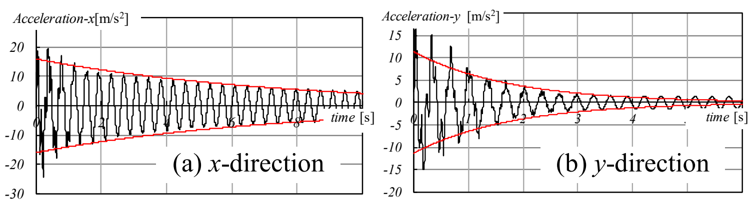


Fig.3 Free vibration test of L4000 model

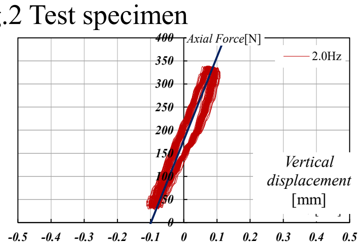


Fig.4 Vertical property



 

## 2.2 Dynamic instability behavior of hanging bolt

A shaking table test in which a sweep wave was input in the vertical direction was conducted in order to experimentally examine frequency when the hanging bolt becomes unstable. The frequency region of input sweep wave here is set at 1.8-4.0 Hz for *L4000* and 2.5-4.8 Hz for *L4000w* model so as to cover the unstable region obtained from the Mathieu equation.

Figures 5-8 show the experimental results (response acceleration in the vertical direction ($z$) at ceiling surface, response acceleration in the horizontal direction ($x,y$) at the center of hanging bolt and axial force on hanging bolt) of *L4000w* model with an input acceleration of 8 m/s$^2$. Each horizontal axis in these figures is not the time but the frequency of the input wave. Since the sweep wave used in this chapter is "Linear sweep" wave and frequency is a linear function of time, the horizontal axis of time history can be represented by the frequency. The dashed red lines in Figure 5 indicate the amplitude ($\pm$8m/s$^2$) of the input acceleration. And the peak value of experimental response acceleration agrees with the dashed line in the region from the initial stage to the point where the frequency of the input wave reaches 3.1Hz. The reason why the response acceleration of the ceiling surface coincides with the amplitude of the input acceleration is that the hanging bolt behaves almost as a rigid body because the vertical natural frequency of the hanging bolt is much higher than the frequency of the input wave. This means that the experiment was performed correctly. However, after that, a response acceleration on the ceiling surface becomes much larger than the input acceleration. The horizontal accelerations at the center of hanging bolt shown in Figures 6-7 also rapidly grow at the same timing, and the maximum value of horizontal accelerations is more than that of vertical acceleration. Such phenomenon, that is, a horizontal response appears without horizontal disturbance is caused by the dynamic instability behavior, as shown by the authors in a previous study using numerical analysis. Figure 8 shows the change in the axial force of the hanging bolt. The dotted and dashed red lines in this figure represent the initial axial force, which is a self-weight of ceiling surface, and the amplitude of axial force ($M_{ceiling}$×8m/s$^2$) calculated from the amplitude of the input acceleration, respectively. And the solid red line represents the vertical strength (1.1kN) of steel furring per one hanging bolt in JPN style ceiling obtained in the previous experiment. Similar to the change in the response acceleration described above, the axial force initially changes in the area defined by the dotted line, which is calculated from the acceleration amplitude centered on the dashed line (indicating

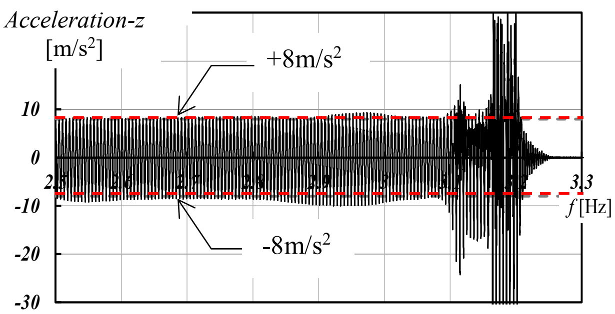


Fig.5 Response acceleration ($z$) on ceiling surface

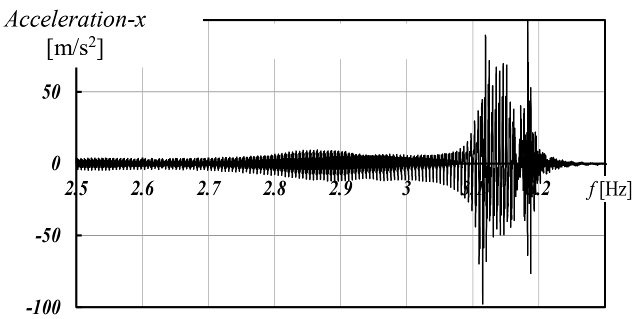


Fig.6 Response acceleration ($x$) at center of hanging bolt

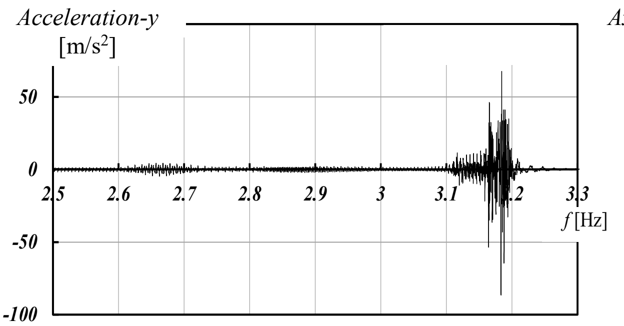


Fig.7 Response acceleration ($y$) at center of hanging bolt

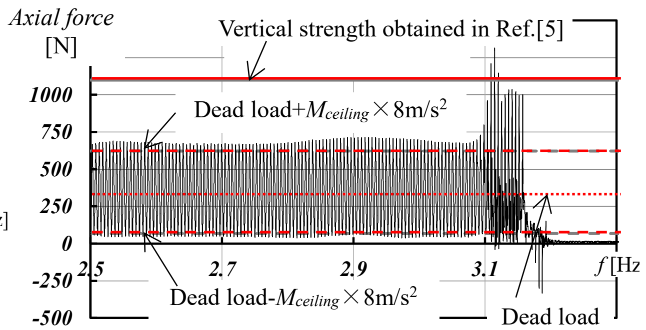


Fig.8 Axial force on hanging bolt including dead load



 

its own weight), but when lateral vibration occurs due to the dynamic unstable behavior of the hanging bolt after 3.1 Hz, the axial force on the hanging bolt varies in a complicated manner. In this experiment, the ceiling surface dropped after the axial force of the hanging bolt exceeded the red solid line indicating the vertical strength. Figure 9 shows the relationship between the axial force of the hanging bolt and the horizontal displacement at the center of the hanging bolt in each input frequency stage. Here, the three stages are shown individually. The colored line is the result in each frequency range. (a) Stable stage: The axial force of the hanging bolt is in the expected range described above (the red colored area in the figure), and the hanging bolt is hardly displaced in the horizontal direction. (b) Transition stage; displacement in the horizontal direction occurs gradually, but has only a little effect on the axial force. (c) Unstable stage: The horizontal displacement is growing rapidly, and the fluctuation of the axial force is increasing rapidly.

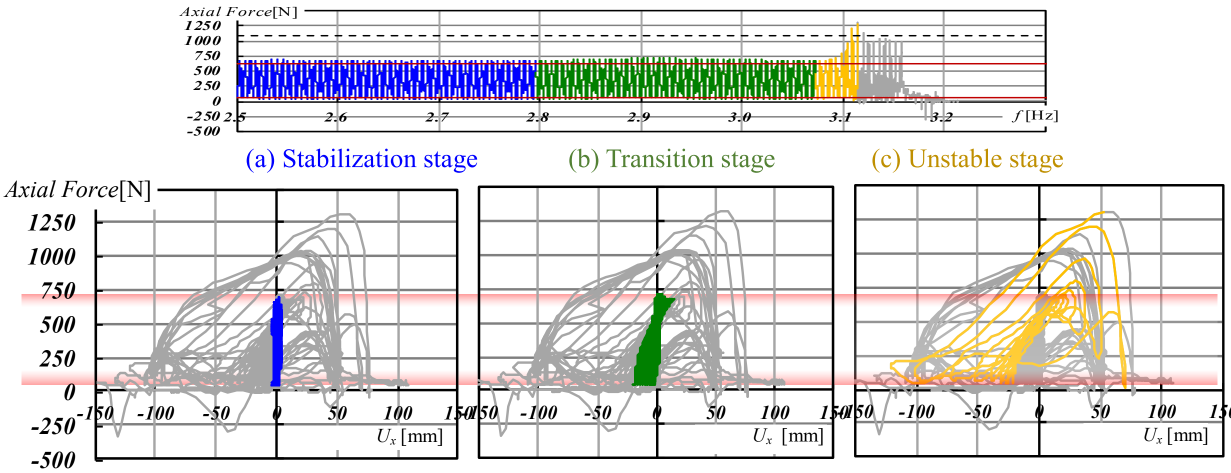


Fig.9 Relationship between axial force and horizontal displacement

Figures 10 show Fourier amplitude spectra of the response acceleration in $x$ directions at the center of one hanging bolt in *L4000w* model in case of input acceleration with 0.5, 0.7 and 0.8 times of the gravitational acceleration. As the input acceleration increases, a response in the horizontal direction appears even at a frequency lower than the natural frequency 3.45Hz. This phenomenon can be explained using the Strutt diagram. Figures 11 are Strutt diagrams and solid black lines show boundary of unstable region for the damping constants $h$=0.8%. The vertical axis represents the magnitude of the input acceleration divided by the gravitational acceleration $g$, and the horizontal axis represents the frequency of the input acceleration ($f_{input}$). The frequency estimated as an unstable region from Strutt diagrams in Figure 11 almost coincides with the frequency at which the response starts to be amplified in Figure 10. This means that it is possible to predict the occurrence of dynamic instability of the hanging bolt by using the Strutt diagram.

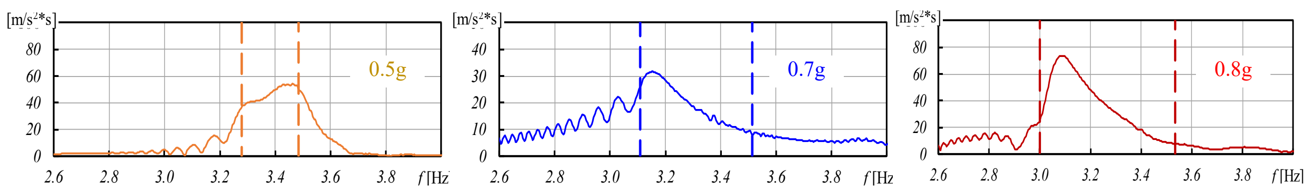


Fig.10 Fourier spectra of horizontal acceleration at center of bolt

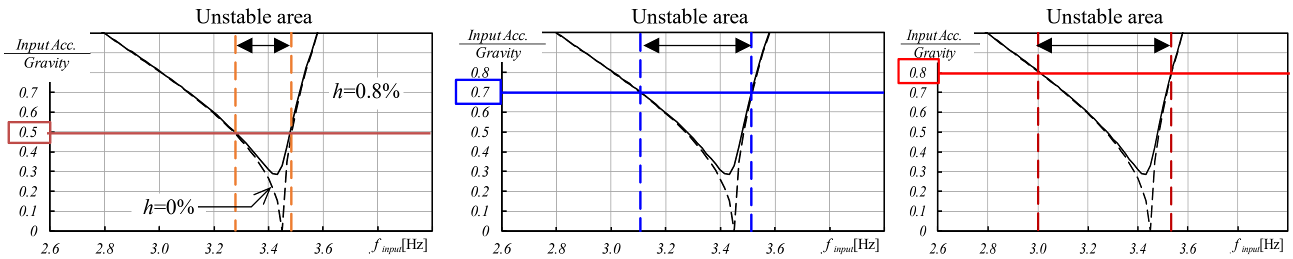


Fig.11 Unstable region for each input accleration based on Strutt diagram



 

## 3. Ceiling with long hanging bolts subject to horizontal dynamic disturbance

### 3.1 Shaking table test of ceiling with long hanging bolts

In this section, we first experimentally investigate the behavior of a ceiling system with long hanging bolts subjected to horizontal dynamic disturbances, and examine whether the same behavior as the dynamic unstable phenomenon of hanging bolts observed during vertical disturbances appears. Particularly, we focus on whether large fluctuations of axial force on the hanging bolts, which are considered to have ~~a~~ great influence on ceiling falling, occur during horizontal disturbances.

Figure 12 shows a test apparatus. The size of the ceiling surface of the test piece is 1.5m x 4.8m. In order to represent a ceiling system without artificial gaps between the ceiling surface and surrounding elements such as walls, a surrounding beam is arranged and the ceiling surface is installed so as to be in contact with it. The ceiling surface is a two-layered (Ceiling A) or three-layered specification (Ceiling B) with 9.5mm-thick boards. A two-layered ceiling is one of the most common specification, and a three-layered one is less common in general, but is sometimes used for auditoriums. The standard steel furring in JPN style ceiling is used in both ceilings. The total mass of the ceiling surface, the mass per hanging bolt are;

| | Total mass | Mass per one hanging bolt |
|---|---|---|
| Ceiling A | 108.3 kg (= 15.0 kg / m2 × 7.2m$^2$) | 10.2 kg / piece (= 108.3 kg / 12 pieces) |
| Ceiling B | 155.2 kg (= 21.6 kg / m2 × 7.2 m$^2$) | 14.5 kg / piece (= 155.2 kg / 12 pieces) |

The length of every hanging bolts is 2,950mm and the boundary condition at the top of them is pinned support. Hanging bolts of 12.5mm outer diameter are applied to both test specimen though general JPN ceiling system has 9mm outer-diameter hanging bolts. Furthermore, an additional mass of 300g is attached to the

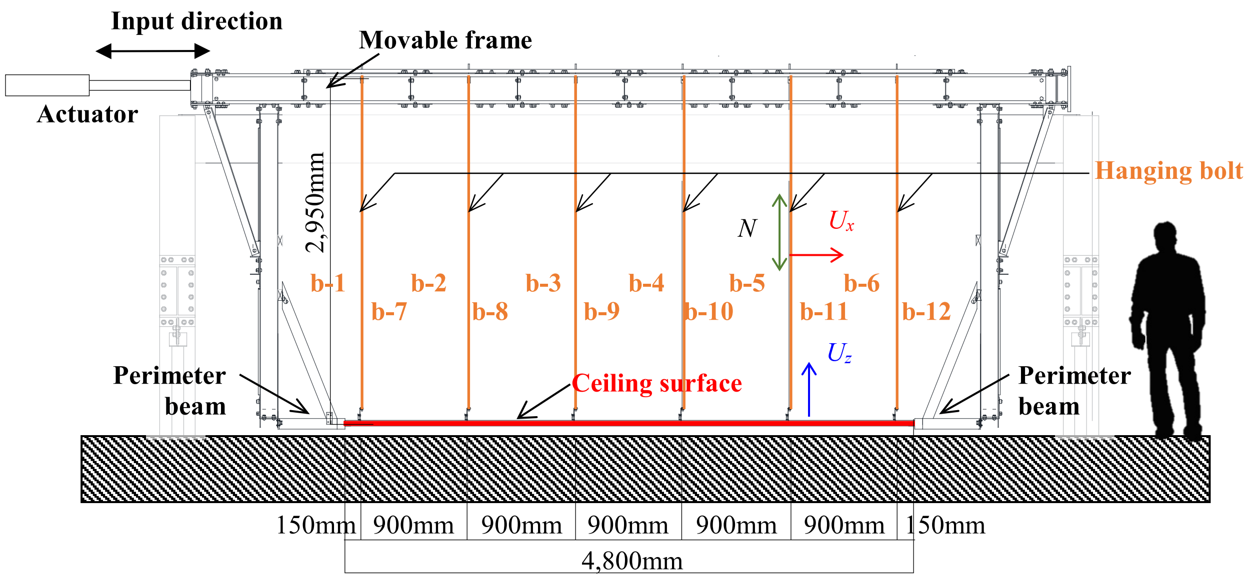


Figure 12 Shaking table test

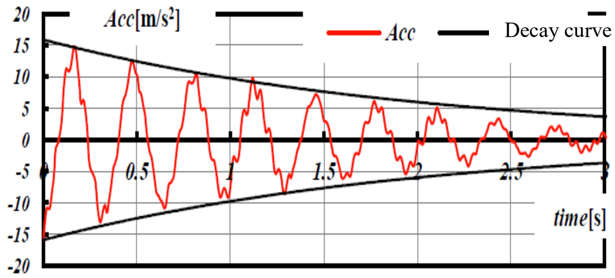


Figure 13 Free vibration test

Table 1 natural frequency of hanging bolts

| Ceiling A | b-1 | b-2 | b-3 | b-4 | b-5 | b-6 | b-7 | b-8 | b-9 | b-10 | b-11 | b-12 |
|---|---|---|---|---|---|---|---|---|---|---|---|---|
| $f_{bolt}$ [Hz] | 2.64 | 3.36 | 3.13 | 3.10 | 3.10 | 2.97 | 2.92 | 3.34 | 2.42 | 3.72 | 2.96 | 2.91 |
| $h$ [%] | 1.60 | 3.00 | 2.70 | 2.50 | 2.60 | 2.00 | 2.00 | 1.00 | 1.50 | 2.40 | 2.40 | 1.80 |
| Ceiling B | b-1 | b-2 | b-3 | b-4 | b-5 | b-6 | b-7 | b-8 | b-9 | b-10 | b-11 | b-12 |
| $f_{bolt}$ [Hz] | 2.69 | 3.36 | 3.08 | 2.97 | 3.27 | 2.86 | 2.96 | 3.13 | 2.97 | 3.49 | 2.92 | 2.98 |
| $h$ [%] | 2.40 | 2.40 | 2.50 | 0.80 | 3.80 | 3.00 | 2.00 | 1.60 | 2.00 | 1.10 | 2.30 | 2.50 |



 

center of all hanging bolts in Ceiling B to reduce natural frequency of the hanging bolts. The reason of making the natural period of the hanging bolt as high as possible is to be described later in this section. In order to find the natural frequency of each hanging bolt, free vibration tests were performed. Figure 13 shows an example of the response acceleration. The bolt-4 in Ceiling A has natural frequency 3.1Hz and damping ration 2.5%. The damping ratio *h* is obtained by the same method in Section 2. Table 1 shows the natural period and damping ratio of all the hanging bolts. The target acceleration input to the shaking table and its Fourier amplitude spectrum are shown in Figure 14 and 15. The acceleration is a sweep wave whose frequency changes from 0.8 Hz to 1.6 Hz. The amplitude is constant after reaching the target value in the first 10 seconds from the start. Figures 16 and 17 show the acceleration actually measured on the shaking table and its Fourier amplitude spectrum. Comparing Figure 14 with Figure 16, the maximum value of the measured acceleration is two times of the amplitude of the target acceleration. In the spectrum corresponding to the measured acceleration shown in Figure 17, a peak at around 2.4 Hz which is not seen in the spectrum of the target wave in Figure 15, is observed. This is considered to be noise generated due to the characteristics of the shaking table, and it is worrisome that the noise adversely affect the experiment. The reason why the natural frequency is made as small as possible is to minimize the influence of the characteristics of the shaking table.

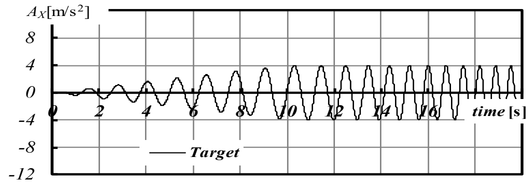


Figure 14 Taget input sweep wave

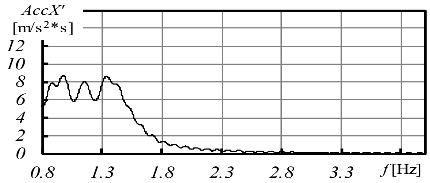


Figure 15 Fourier spectrum of target wave

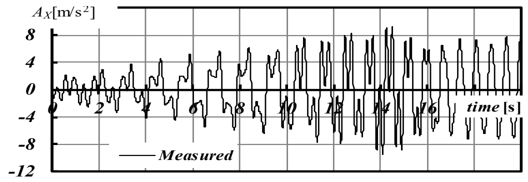


Figure 16 Measured acc on shaking table

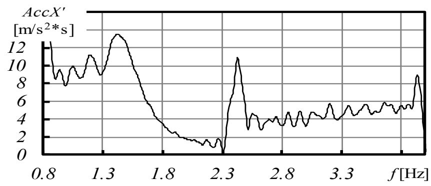


Figure 17 Fourier spectrum of meassured wave

Figure 18 shows the test results of Bolt-5 in Ceiling A. The upper graph shows the displacement of the center point of the hanging bolt in the X direction, the middle graph shows the vertical displacement of the ceiling surface (the lower end of the hanging bolt), and the lower graph shows the axial force of the hanging bolt. The axial force in Figure 18 (c) includes the mass per one hanging bolt described above, that is, the self-weight of the ceiling surface. The top and bottom horizontal axes of each graph are time and frequency of input wave at that time. The response of horizontal displacement, vertical displacement and axial force on the bolt

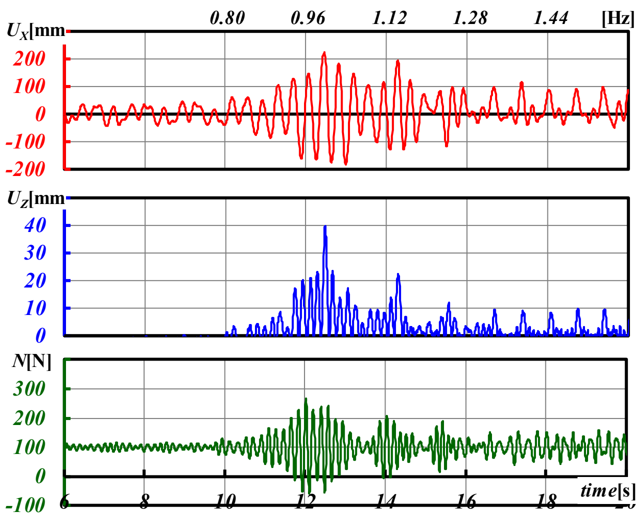


Figure 18 Test results of Ceiling A

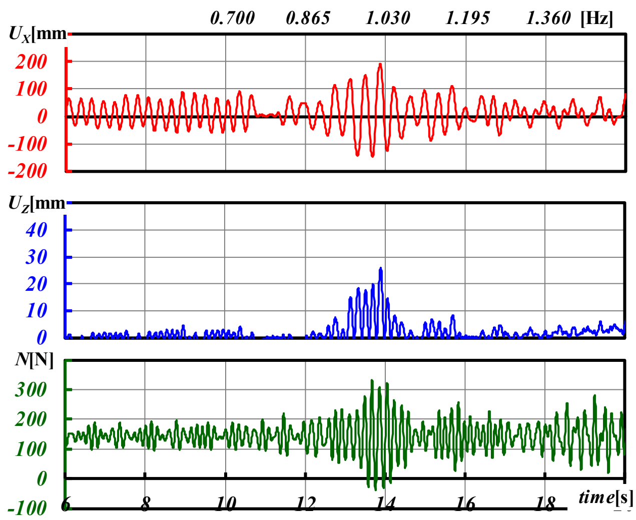


Figure 19 Test results of Ceiling B



 

hardly appears for about 10 seconds until the amplitude of the input acceleration reaches 4 m/s2 from the start of the test. After 10 seconds, the horizontal and vertical displacements begin to increase sharply, and the axial force of the bolt also greatly changes. The frequency of the input acceleration at this time is 0.96 Hz, and this value is significantly different from the natural frequency about 3 Hz, obtained by the free vibration test of the hanging bolt (See Table 1). As shown in Figure 19, the results of the ceiling B are almost the same as the ones of Ceiling A.

## 3.2 Numerical model for dynamic behavior of ceiling with long hanging bolts

In Section 3.1, it has been observed that the resonance phenomenon of the hanging bolt begins to occur in a frequency range considerably lower than the natural frequency of the hanging bolt. The above-mentioned noise which is generated by the shaking table can be considered as one of the causes, but it cannot be specified only by experimental results. Therefore, numerical analysis is performed to clarify the inevitability of this phenomenon. In this numerical analysis, only a single hanging bolt is extracted. Figures 20 and 21 show the temporal and spatial variations of the vertical displacement at the ceiling surface just below the hanging bolts to verify the validity of extracting this single bolt. The former is the time history of the vertical displacement at each hanging bolt position and the latter is its spatial distribution. From these figures, it is clear that the vertical displacement at each point on the ceiling surface is substantially equal, and it can be seen that the ceiling surface is moving almost as a rigid body. This fact means that modeling to extract a single hanging bolt is appropriate. The numerical analysis model is shown in Figure 22 and the specifications of the hanging bolt are as shown in Table 2. Since the ceiling surface can be assumed to be a rigid body, the value shown in Table 1 is adopted as the mass at the bottom end of the bolt in this model. On the boundary condition, the top and bottom ends of the hanging bolt are pinned and rollered supports respectively. The natural frequency calculated with numerical analysis using this model almost agrees with the experimental result, while the boundary

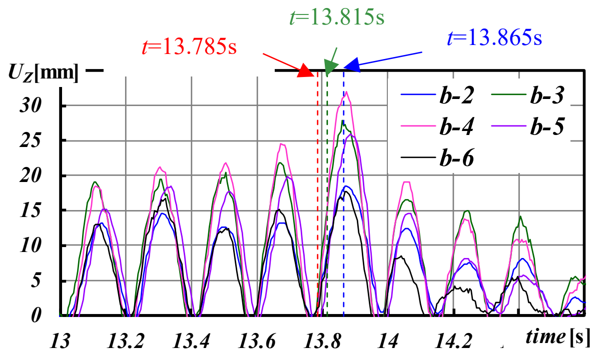


Figure 20 Time history of vertical displacement at ceil

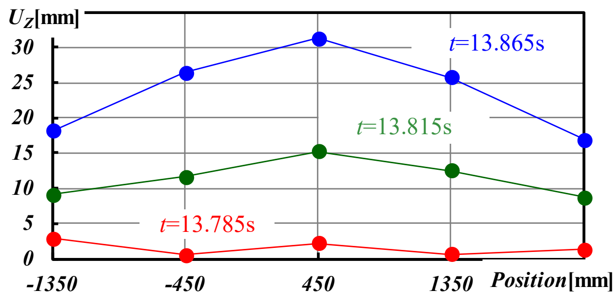


Figure 21 Distribution of vertical displacement at ceiling

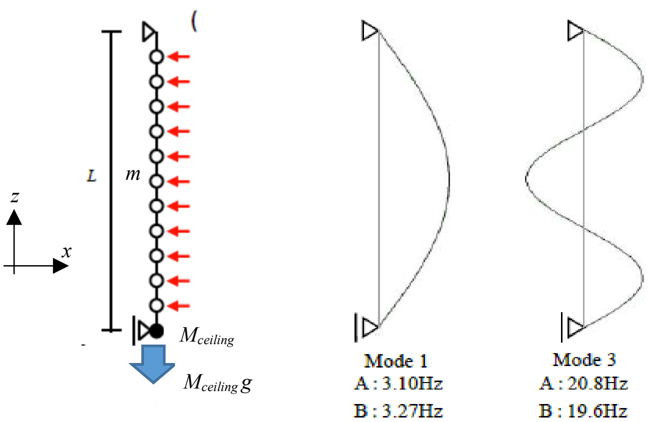


Figure 22 Numerical model

Table 2 Poperties of hanging bolt

| | | | |
|---|---|---|---|
| Length | $L$ | 2950 | mm |
| Young's modulus | $E$ | 2.05E+05 | N/mm$^2$ |
| Section area | $A$ | 85.1 | mm$^2$ |
| Mass per unit length | $m$ | 8.20E-04 | kg/mm |
| Moment of Inertia | $I$ | 576.4 | mm$^4$ |
| Initial tension | $N_0$ | 117.7 (A)<br>225.5 (B) | N |



 

condition of the hanging bolt in numerical model differs from the actual one. This is because the influence of the boundary condition on the natural frequency is reduced when the length of the hanging bolt is long. As an input acceleration, we adopt the acceleration measured in the shaking table test shown in Figure 16. Figure 23 shows the horizontal displacement at the center of the hanging bolt (top), the vertical displacement at the bottom end of the hanging bolt (middle), and the axial force of the hanging bolt (bottom) by numerical analysis, and Figure 24 shows the relationship between the axial force and the vertical / horizontal displacement. In the both figures the experimental results are also presented. From these figures, it is confirmed that the numerical analysis results are in good agreement with the experimental results. This means that the strange phenomenon observed in the experimental results is inevitable and true, and that the present numerical model is also valid.

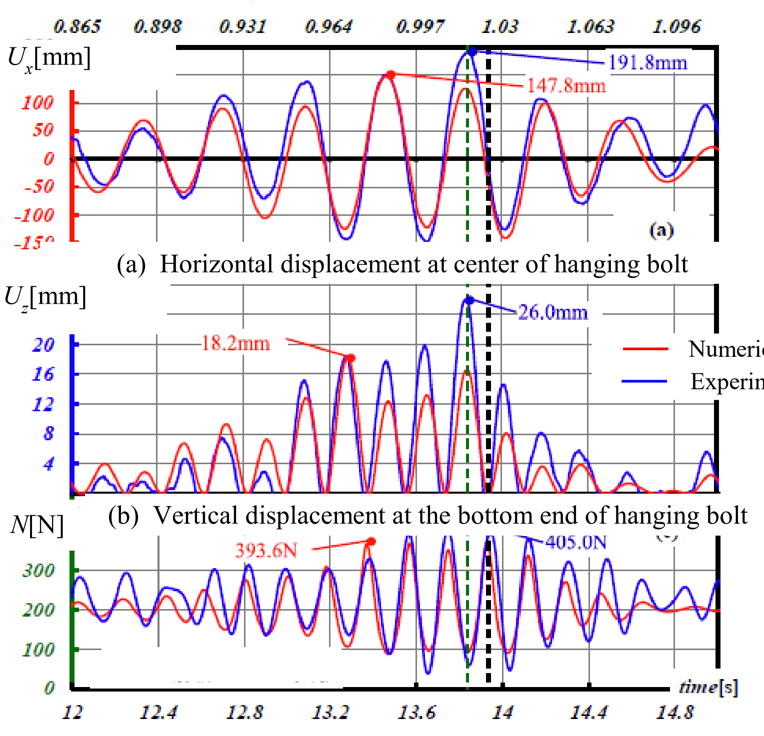

(a) Horizontal displacement at center of hanging bolt

(b) Vertical displacement at the bottom end of hanging bolt

(c) Axial force on hanging bolt

Figure 23 Comparison between numerical and experimental results

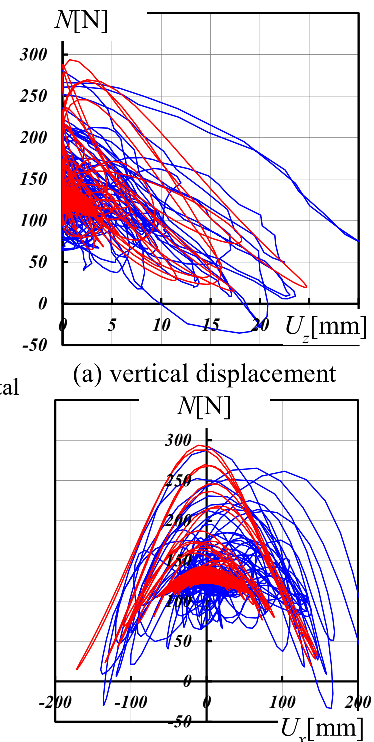

(a) vertical displacement

(b) Horizontal displacement

Figure 24 Axial force vs displacement

## 3.3 Effect of magnitude of input acceleration and mass of ceiling surface on behavior of hanging bolt

Using the present numerical model, we hereafter verify numerically the effects of magnitude of input acceleration and the mass of ceiling surface on the dynamic behavior of a hanging bolt.

First, the effect of the magnitude of the input acceleration is discussed here. The input acceleration is a sweep wave with 2 Hz to 4 Hz including the natural frequency of the hanging bolt, the amplitude of sweep wave is constant from 100 cm/s$^2$ to 1500 cm/s$^2$. Figure 25 shows examples (100, 500, 1000 cm/s2) of the axial force on the hanging bolt obtained by numerical analysis. Note that, similar to Section 2, since a linear sweep wave is used, the horizontal axis of the graph uses the input frequency instead of time. At the input acceleration of 100cm/s$^2$ indicated by the green line, the resonance phenomenon of the hanging bolt is observed when the input frequency corresponds to the natural frequency of the hanging bolt. On the other hand, when the amplitude of the acceleration increases, the maximum value of the axial force is observed at an input frequency considerably lower than the natural frequency. That is, the frequency 2.7 Hz for 500 cm/s$^2$ and 2.45 Hz for 1000 cm/s$^2$. This is because when the horizontal response displacement to horizontal disturbance becomes larger than a certain level, vertical response displacement and response acceleration at the bottom end of hanging bolt occur due to the influence of geometric nonlinearity, and this vertical acceleration causes the similar phenomenon as the dynamic instability shown in the previous section. As a result, the frequency at the point where axial force begins to change is lower than the natural frequency as shown in the Strutt diagram of Figure 11.

Figure 26 shows the relationship between the magnitude of the input acceleration and the maximum value (tensile force) of the axial force on the hanging bolt. As the input acceleration increases, the tensile force increases linearly. In this example, when the magnitude of the input acceleration is approximately 1,200 cm/s$^2$, the axial force on the hanging bolt reaches 1.1kN, the value is the tensile (falling) strength of the ceiling surface. As a result, the ceiling surface falls. The magnitude of the input acceleration of 1,200 cm/s$^2$ is a magnitude that can be conceivable during an actual earthquake because the response acceleration of the building is the input acceleration for non-structural elements.

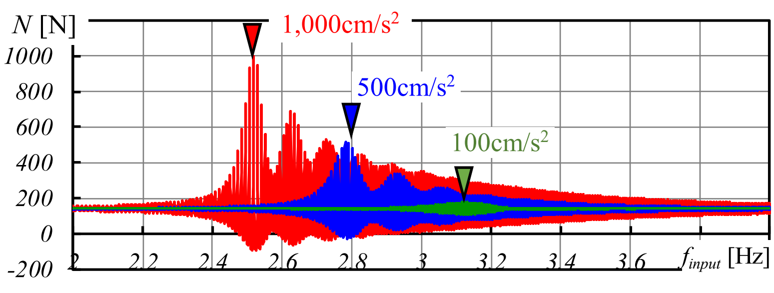


Figure 25 Time hstory of axial force on hanging bolt

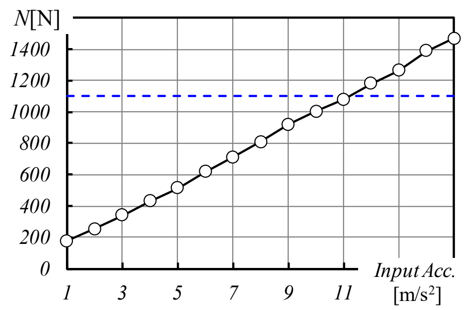


Figure 26 Influence of magnitude of input acceleration on axial force on hanging bolt

Now, the effect of the mass of the ceiling surface is to be described here. With the properties of a hanging bolt including its mass being constant, three kinds of ceiling surface (mass being 20, 12, 5 kg/m$^2$ are considered and the influence on the behavior of hanging bolts is examined. First, we would like to consider the effect of the mass of ceiling surface on the natural frequency of hanging bolts. As is clear from the formula shown in Eq.(1) of the natural frequency for the bending member subjected to the axial force, when the mass of ceiling surface increases, the apparent lateral stiffness of hanging bolt increases as the axial force on the hanging bolt gets bigger, and as a result, the natural frequency of the hanging bolt becomes higher.

$$f_{bolt}(EI,m,L,N_0)=\frac{\pi}{2L^2}\sqrt{\frac{EI}{m}\left(1+\frac{N_0}{N_{cr}}\right)}, \qquad N_{cr}=\frac{\pi^2 EI}{L^2} \tag{1}$$

where $f_{bolt}, EI, m, L, N_0$ are a natural frequency, bending rigidity, mass per unit length, total length and initial axial force see Table 2. The natural frequency of the hanging bolt by eigenvalue analysis using this numerical analysis model is calculated as follows: 2.56Hz at the mass of the ceiling surface of 5kg/m$^2$, 3.01Hz at 12kg/m$^2$, and 3.44Hz at 20kg/m$^2$. These values are surely consistent with the results from Eq.(1). However, the word 'mass' used here is not strictly correct, because it is the weight of the ceiling surface that affects the natural frequency of the hanging bolt, not the mass. The input acceleration is a sweep wave having the same frequency as the analysis described above. Its amplitude is set at 500m/s$^2$ throughout. Figures 27 shows the numerical results. As mentioned above, when the mass of the ceiling surface increases, the apparent lateral stiffness of the hanging bolts increases, so it is generally considered that the horizontal response displacement for the same input acceleration decreases. The present numerical results agree with this consideration. However, it seems that the variation in the axial force of the hanging bolt has no direct correlation with the increase in the response displacement. In Figure 27(c), the amplitude of the axial force for Ceiling 20 is the largest while displacement responses for the model are the smallest. This is because the axial tension in Figure 27 (c) does not include the initial tension due to the ceiling surface weight. The initial tension at each ceiling mass is 49N, 117.6N and 196N, and the true axial forces on hanging bolt are obtained by adding these. Table 3 summarizes the amount of axial force fluctuation. $N_0$, $\Delta N_{comp}$, $\Delta N_{ten}$, $C_{max}$, and $T_{max}$ are the initial axial force, the maximum fluctuation values on the compression side or the tension side, the maximum compression force (initial tension +



 

fluctuation value on compression side), and the maximum tensile force (initial tension + fluctuation value on tension side). For the maximum tensile force $T_{max}$, the ratio of the maximum tensile force to the initial tension $R_{ten}$ ((variation amount + initial tension) / initial tension) is also written for easy understanding. The value of the maximum compression force $C_{max}$ is the largest in Ceiling 5 of which mass is the smallest. On the other hand, the value of the maximum tensile force is determined by product of $R_{ten}$ and $N_0$, and $N_0$ has a positive correlation with $M_{ceiling}$ and $R_{ten}$ has a negative correlation with it respectively. Therefore, the maximum tensile force strongly depends on the response of the hanging bolt and can not be estimated easily. However, from the results, it is qualitatively certain that a large fluctuation of axial force due to the geometric nonlinearity occurs in a ceiling with long hanging bolts and heavy ceiling surface, and such ceilings easily fall during earthquakes.

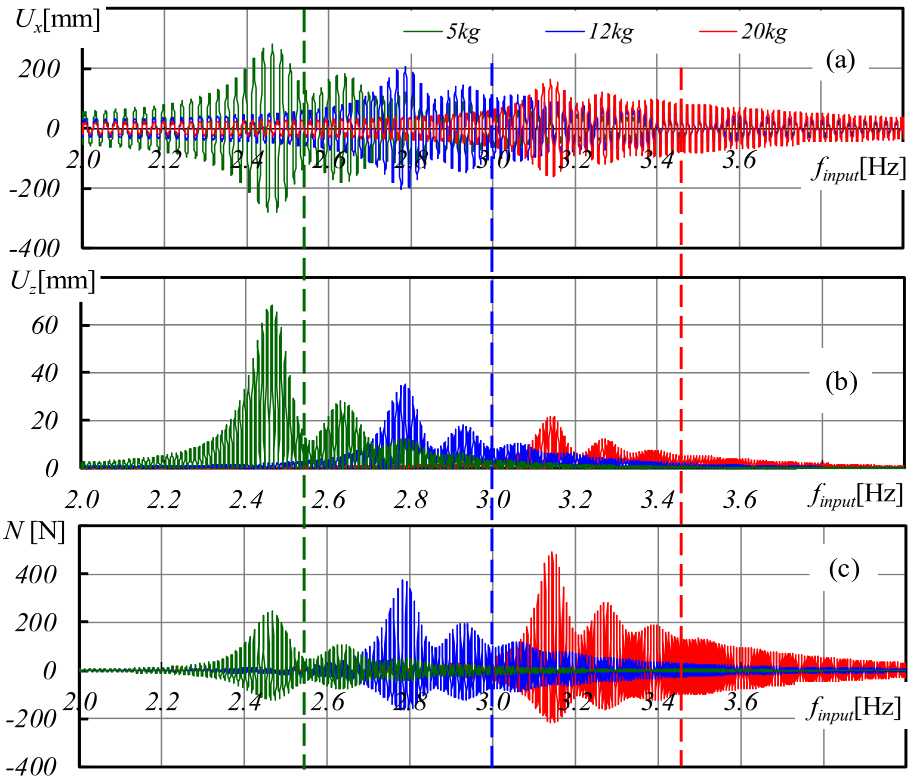


(a) Time history of horizontal displacement at center of hanging bolt
(b) Time history of vertical displacement on ceiling surface
(c) Time history of axial force on hanging bolt

Figure 26 Influence of ceiling surface mass

Table 3 Summary of test results

| *Model name* | Ceiling 20 | Ceiling 12 | Ceiling 5 |
|---|---|---|---|
| $M_{ceiling}$ | 20kg | 12kg | 5kg |
| $N_0$ | 196N | 118N | 49N |
| $\Delta N_{comp}$ | -205N | -150N | -100N |
| $\Delta N_{ten}$ | 300N | 400N | 250N |
| $C_{max}$ | -5N | -30N | -50N |
| $T_{max}$ ($R_{ten}=T_{max}/N0$) | 500N (2.5) | 520N (4.3) | 300N (6.0) |



 

## 4. Conclusion

In this paper, we have shown through experimental results that nonlinear behavior can actually occur in the longer hanging bolts in a ceiling system during dynamic disturbance, which has been shown only by numerical analysis so far.

In particular, the dropping behavior of the ceiling surface was confirmed by experiments using test specimens that faithfully represented realistic connection conditions by adopting realistic details from the conditions of hanging bolt ends that were assumed to be simply supported in numerical model. This is the first time that it has been done.

Furthermore, through the experimental and numerical examination, the behavior of the hanging bolts shows strong non-linearity even when subjected to horizontal disturbance, and as a result, the axial force generated in the hanging bolts fluctuates greatly, and it is highly likely that the hanging bolt will fall to the ceiling surface.

## 5. Acknowledgements

This work was supported by JSPS KAKENHI Grant Number JP 16H02375 and JST Program on Open Innovation Platform with Enterprises (JPMJOP1723). I am particularly grateful for the assistance given by Rikuro Shimizu and Isao Hirota who were graduate students in Motoyui laboratory.

## 6. References

[1] Shojiro Motoyui, Yasuaki Sato, et.al. (2011): Mechanical characteristics of metal joint parts in Japanese style of ceiling. *8th International Conference on Urban Earthquake Engineering*, Tokyo, Japan.

[2] Shojiro Motoyui, Go Tabuchi, Miyuki Kobayashi Yukihiro Sato and Yasuaki Sato (2012): CEILING DAMAGE BY THE GREAT EAST JAPAN EARTHQUAKE AND ITS RESTORATION, *9th International Conference on Urban Earthquake Engineering/ 4th Asia Conference on Earthquake Engineering*, Tokyo, Japan.

[3] Tadashi Ishihara, et.al.: (2014): Experimental study on seismic performance of ceilings without clearance part 1-5, Proceedings of annual meeting of AIJ, pp.977-986 (in Japanese)

[4] Shojiro Motoyui, Yasuaki Sato (2016): UNSTABLE BEHAVIOR OF SUSPENDED CEILING DURING EARTHQUAKE, *16th World Conference on Earthquake Engineering*, Santiago, Chile.

[5] Shojiro Motoyui, Yasuaki Satoh and Hiroaki Funazumi (2008): Mechanical characteristics of mechanical joint in ceilings part 1-3, *Proceedings of annual meeting of AIJ*, pp.806-811 (in Japanese)



 